# Supporting Information for

## Pseudo-Atomic-Scale Metals Well-Dispersed on Nano-Carbons as Ultra-Low Metal Loading Oxygen-Evolving Electrocatalysts

Jing-Fang Huang* and Wei-Zhe Xie

Department of Chemistry, National Chung Hsing University, Taichung 402, Taiwan, R.O.C.

*Correspondence to: E-mail: jfh@dragon.nchu.edu.tw

**This file includes:**

**The area of single molecule of TA**

The radius of a TA molecule was determined by measuring the length from its center (A) to one of end hydroxyl groups (B). The A-B length was measured to be *ca* 1.28 nm. Thus, the area of single-molecule of TA ($A_{TA}$) is calculated as below.

$A_{TA} = [2 \times (1.28 \times 10^{-9}\ m)]^2 = ca\ 7 \times 10^{-18}\ m^2$

**Coverage of TA on GCE (one monolayer)**

The surface area of GCE/$A_{TA}$ = $7 \times 10^{-6}\ m^2 / 7 \times 10^{-18}\ m^2$

$= \sim 1 \times 10^{12}$ molecules/GCE

$= \sim 1.66 \times 10^{-12}$ moles/GCE

**Coverage of TA on SWCNT (one monolayer)**

<u>The Carbon loading 15.1 μg $cm^{-2}$ is drop-dried on a GCE (0.07 $cm^2$)</u>

➔1.06 μg SWCNT on the GCE and the BET SWCNT specific surface area is about 525 $m^2\ g^{-1}$

⇨ Total surface area of SWCNT on the GCE = $1.06 \times 10^{-6} \times 525 = 5.6 \times 10^{-4}\ m^2$

Coverage of TA on SWCNT (one monolayer):

Total surface area of SWCNT on GCE/ $A_{TA}$ = $5.6 \times 10^{-4}\ m^2 / 7 \times 10^{-18}\ m^2$

$= \sim 8.1 \times 10^{13}$ molecules/GCE

$= \sim 1.33 \times 10^{-10}$ moles/GCE

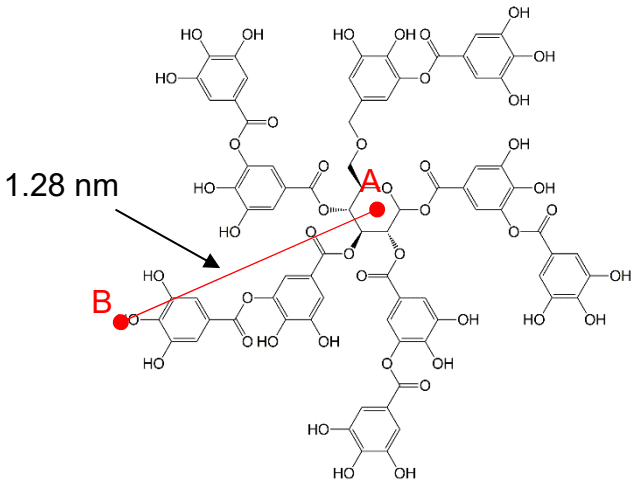


**Fig. S1.** Molecule structure of TA

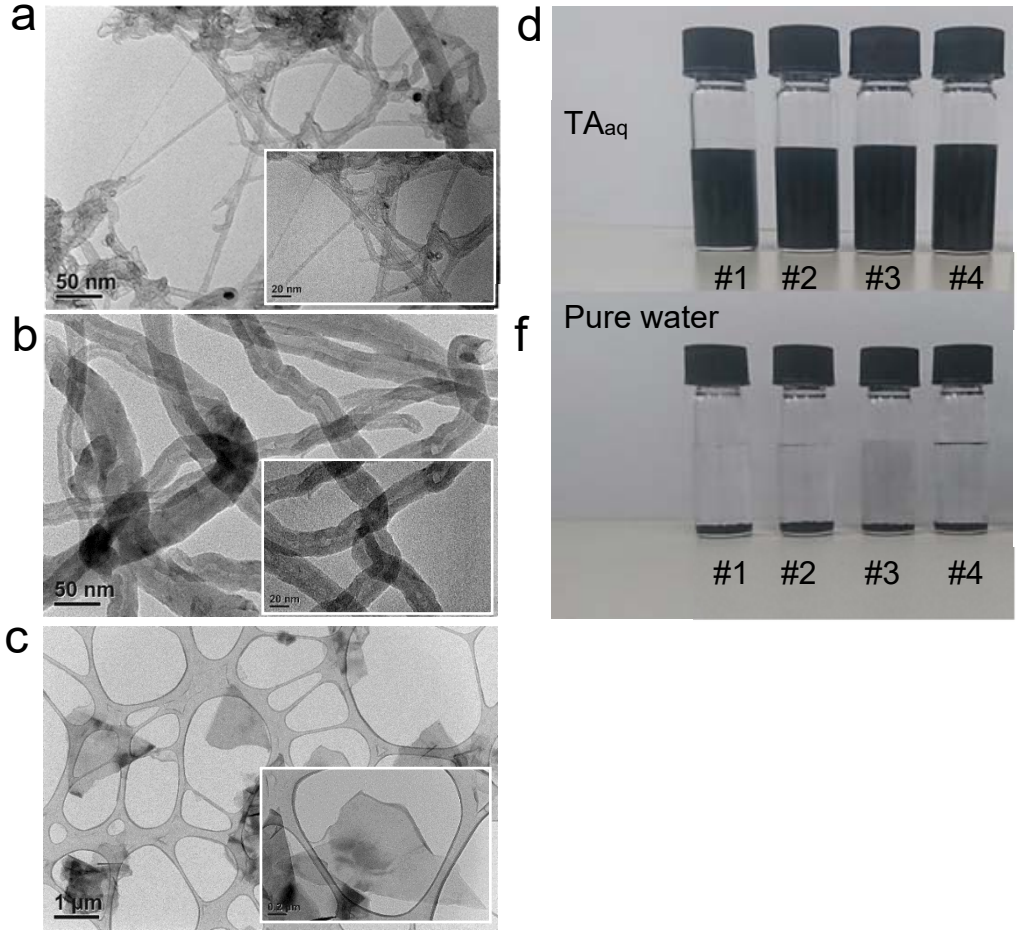


**Fig. S2** TEM images of well-dispersed (a) TA-SWCNT, (b) TA-MWCNT, and (c) TA-GE8; Photographs of vials containing 0.12 wt% NCs, including #1 SWCNT, #2 MWCNT, #3 GE8, and #4 GE12 in (d) 0.12 wt% TA aqueous solution and (e) pure water, respectively.

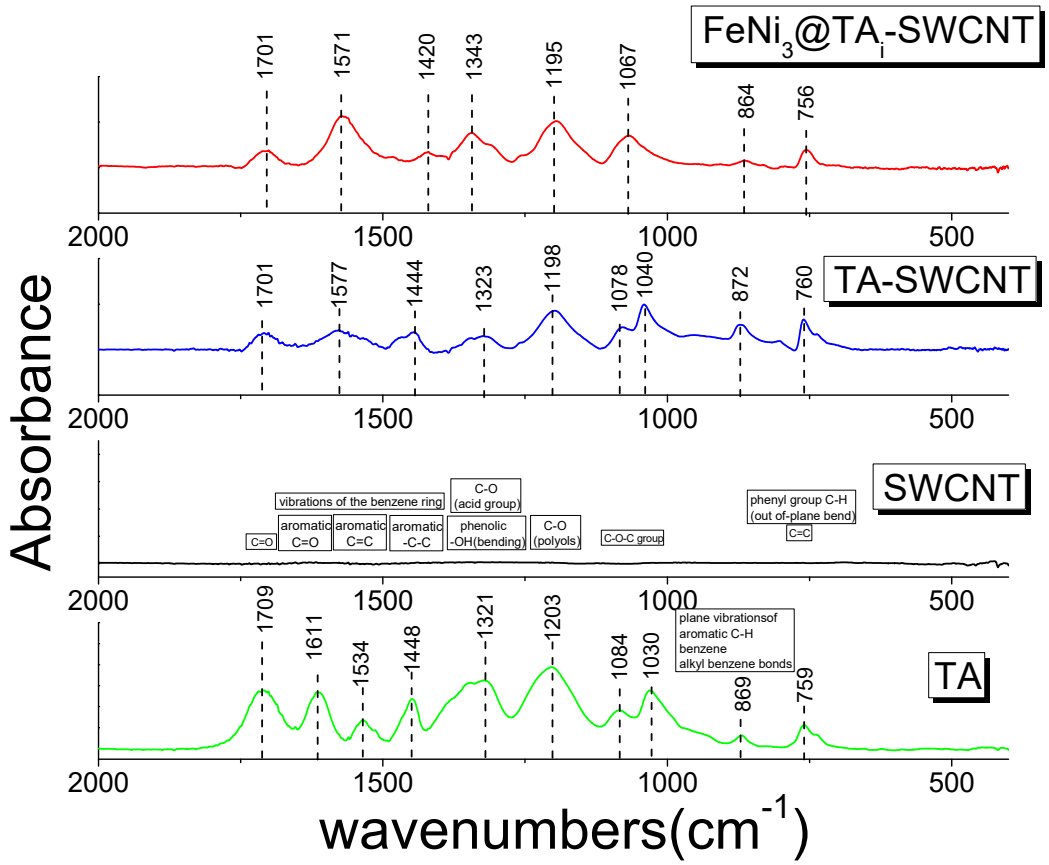


**Fig. S3** FTIR spectra of FeNi3@TAi-SWCNT, TA-SWCNT, SWCNT, and TA.

**pH-controllable TA molecule monolayer on the nano-carbon (NC)**

$TA_{ad}$ on NCs also can be evaluated by CVs recorded in $KOH_{aq}$ (Fig. S4), with $TA_{ad}$ on SWCNT serving as an example. In this case, 4 μl of 0.027 wt% $TA_m$-$SWCNT_{aq}$ (carbon loading 15.1 μg $cm^{-2}$) was drop-dried onto a GCE (0.07 $cm^2$) ($TA_m$-SWCNT@GCE) serving as a working electrode. CVs of TA anodic stripping were recorded after various periods ($t_{de}$) before the CV measurement in 1.0 M $KOH_{aq}$. Anodic waves appear due to TA oxidation to TA-quinone through $2e^-/2H^+$ in the first cycle of CVs, then disappear in the second cycle of CVs, indicating TA anodic stripping from TA-SWCNT. The SWCNT specific surface area is ~525 $m^2$ $g^{-1}$, evaluated from nitrogen adsorption data calculated by the Brunauer-Emmett-Teller method, and is consistent with the data provided by the manufacturer (400–600 $m^2$ $g^{-1}$). $TA_{ad}$ in one monolayer on SWCNT is ~$8.1 \times 10^{13}$ molecules. The $TA_{ad}$ on the as-prepared $TA_m$-SWCNT is ~12 TA molecule layers, which is then reduced to 1–1.5 TA molecule layers after immersion in $KOH_{aq}$ for over 30 min (Fig. S4). These results demonstrate that pH-tunable TA monolayer formation occurs on NCs ($TA_i$-NCs).

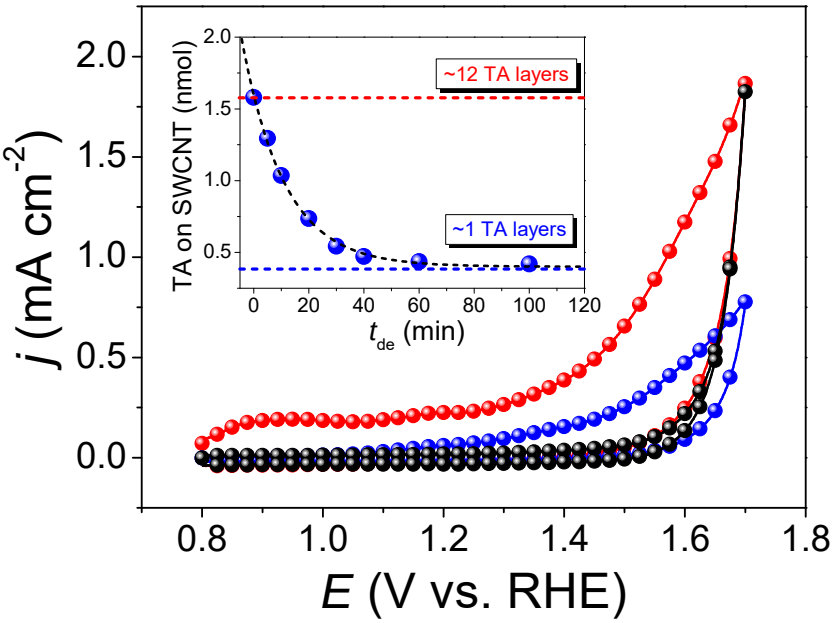


**Fig. S4** CVs of TA anodic stripping were recorded on (black solid circle) a GCE, (red solid circle) a $TA_m$-SWCNT@GCE, and (blue solid circle) a $TA_m$-SWCNT@GCE incubated in 1.0 M $KOH_{aq}$ for $t_{de}$ = 20 min before the CV measurement with a scan rate of 50 mV/s. Inset: $TA_{ad}$ on the TA-SWCNT vs. $t_{de}$.

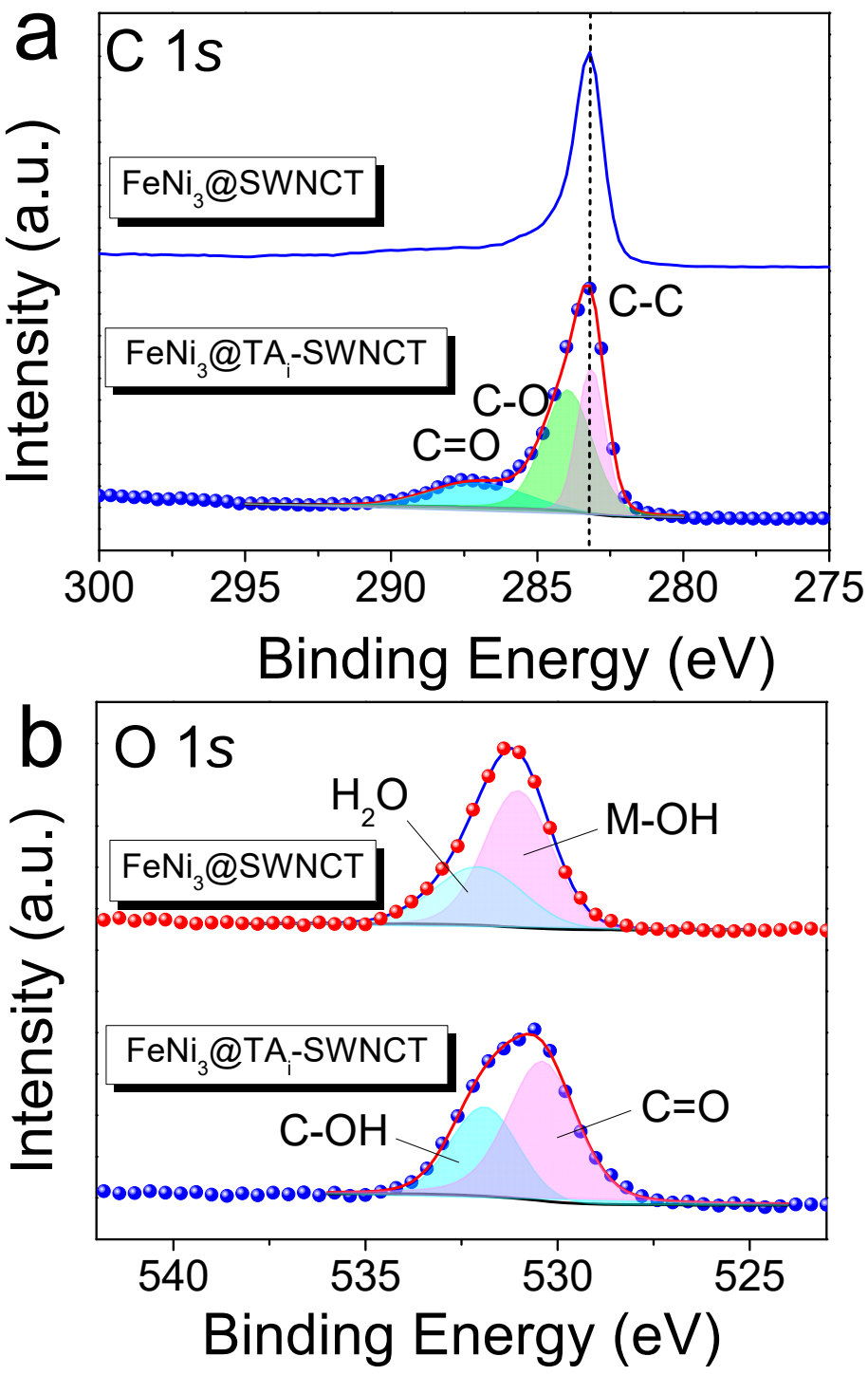


**Fig. S5** C 1*s* and O 1*s* spectra of the FeNi3@SWCNT and FeNi3@TAi-SWCNT.

**UV-Vis of $Fe^{2+}$-TA complex determines the Fe loading on the Fe@SWCNT**

Two peaks of TA were observed at 218 and 275 nm, which correspond to the π–π* and n-π* transitions of TA, respectively (Fig. S6a). After the addition of $Fe^{2+}$, other peaks appeared at 317 and 550 nm. The peak at 317 nm was assigned to the TA absorption peaks coordinated to the $Fe^{2+}$, and the broad peak near 550 nm corresponds to a coordinated TA to $Fe^{2+}$-charge transfer band in the $Fe^{2+}$-TA complex. In the UV-Vis spectra, the absorbance at 550 nm ($A_{550}$) is dependent on the concentration of the $Fe^{2+}$-TA complex (Fig. S6b). The Fe loading on the Fe@SWCNT was determined by tracking the reduction in $A_{550}$ after SWCNT adsorption (Fig. S7).

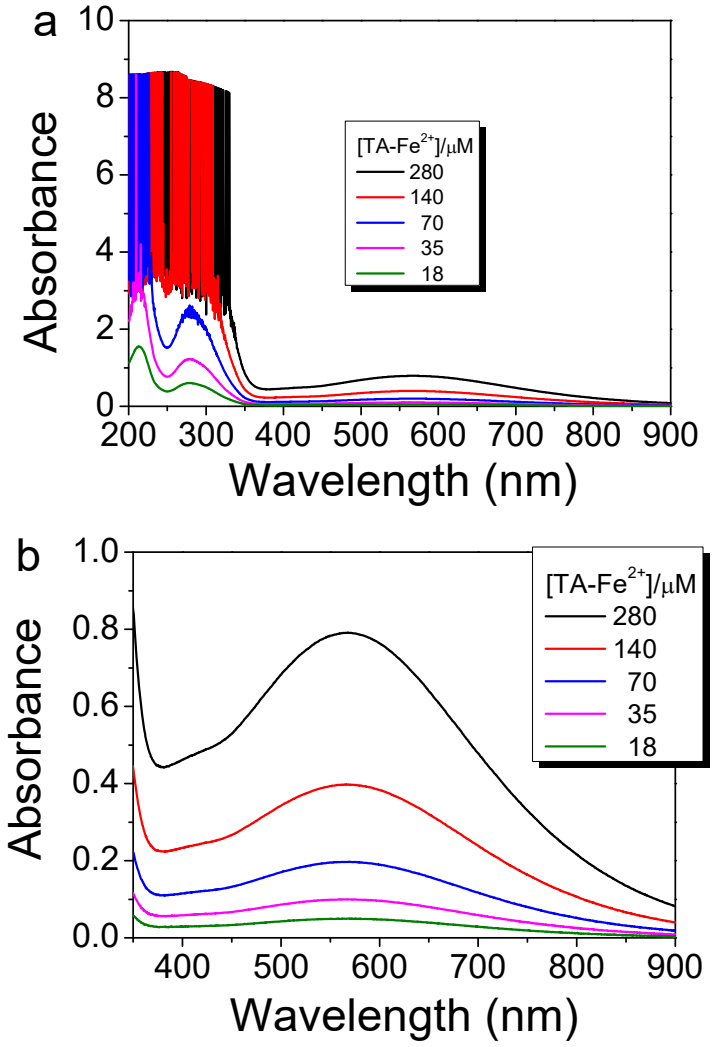


**Fig. S6** UV-Vs absorption spectra a) 200–900 nm and b) 350–900 nm recorded in various of [TA-$Fe^{2+}$].

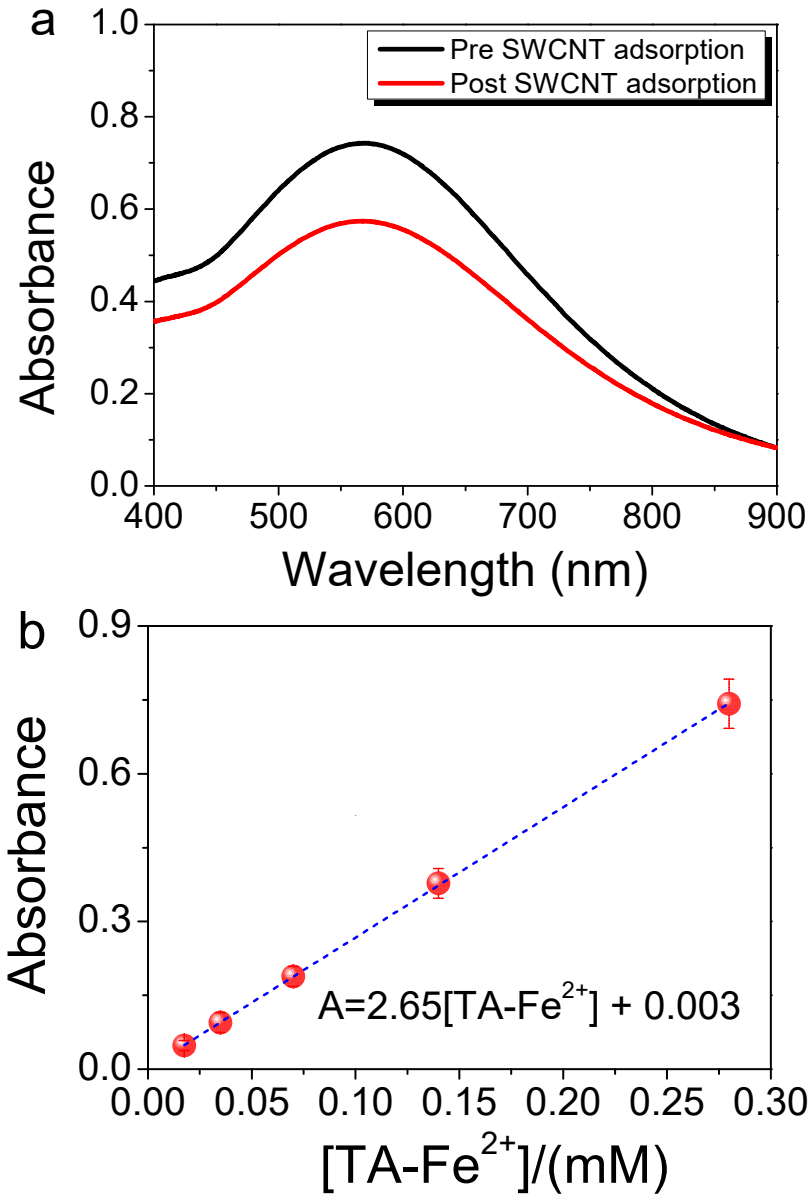


**Fig. S7** (a) Tracking the reduction in $A_{550}$ before and after SWCNT adsorption in TA-$Fe^{2+}$-complex-containing aqueous solution. (b) Calibration curve was recorded as $A_{550}$ vs. [TA-$Fe^{2+}$].

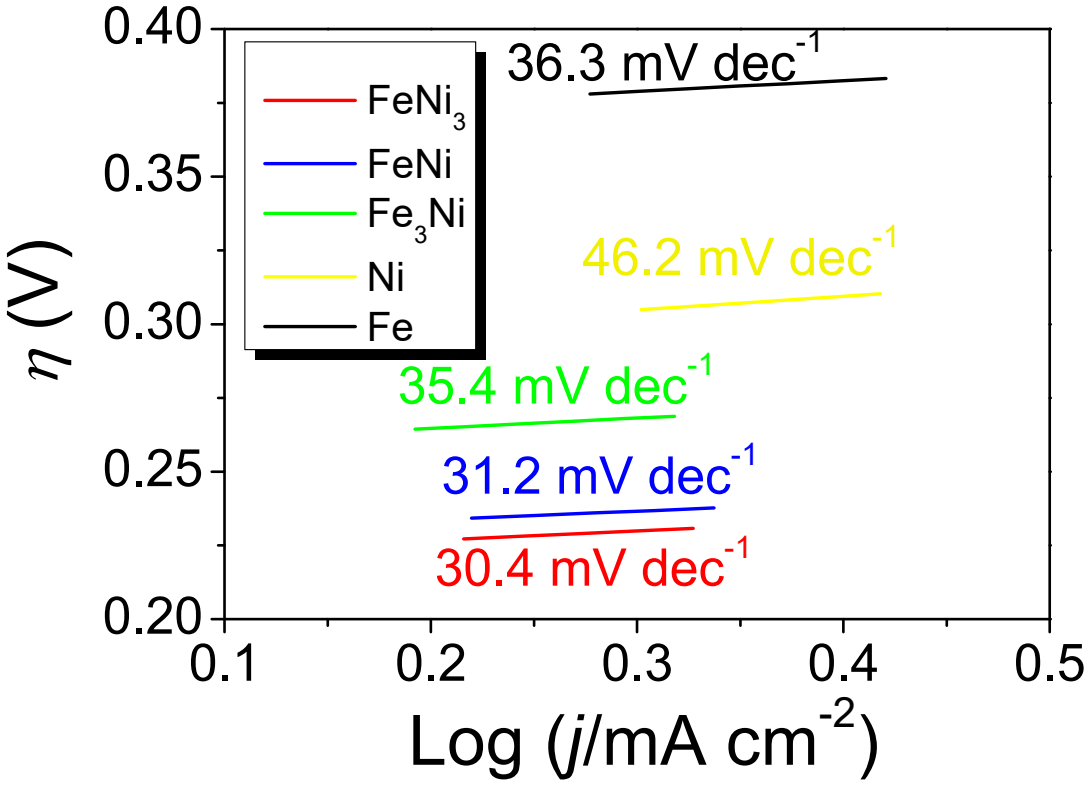


**Fig. S8** Tafel plots are transferred from the data shown in Fig. 6a.

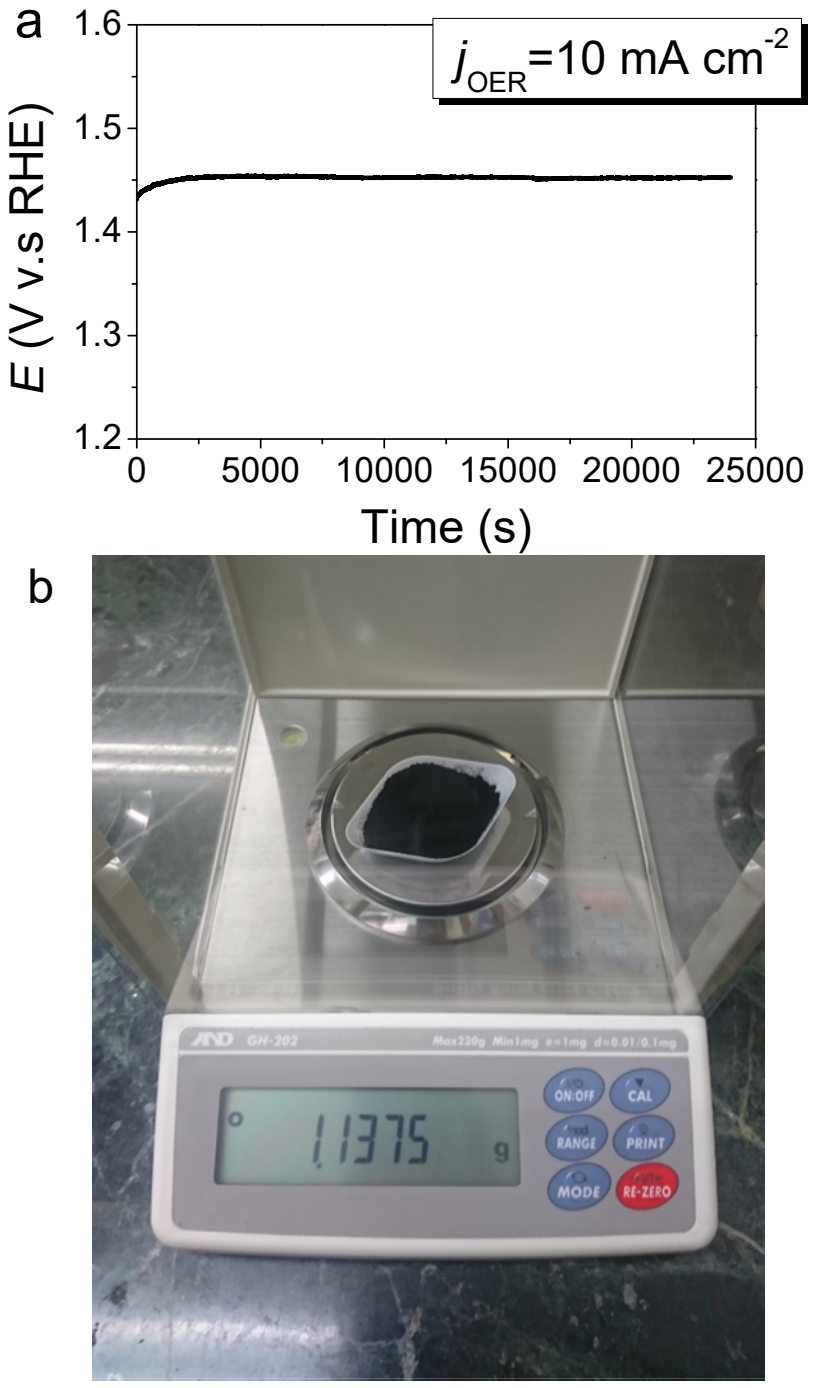


**Fig. S9 (**a) Chronopotentiometry curves at a current density of 10 mAcm$^{-2}$ and (b) gram-scale production of $FeNi_3$@SWCNT.

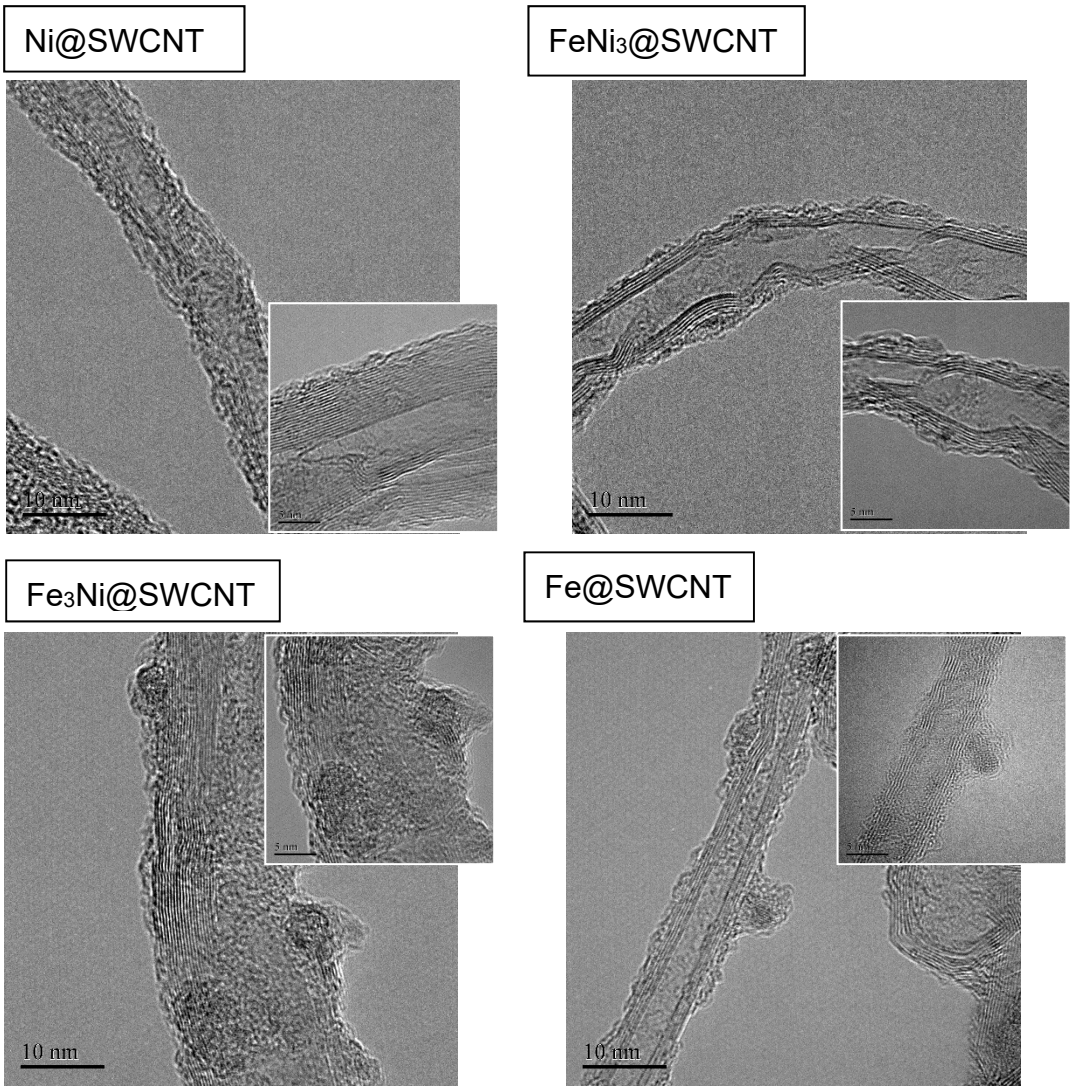


**Fig. S10** HR-TEM images of $(FeNi)_x$@SWCNT including Ni@SWCNT, $FeNi_3$@SWCNT, $Fe_3Ni$@SWCNT, and Fe@SWCNT.

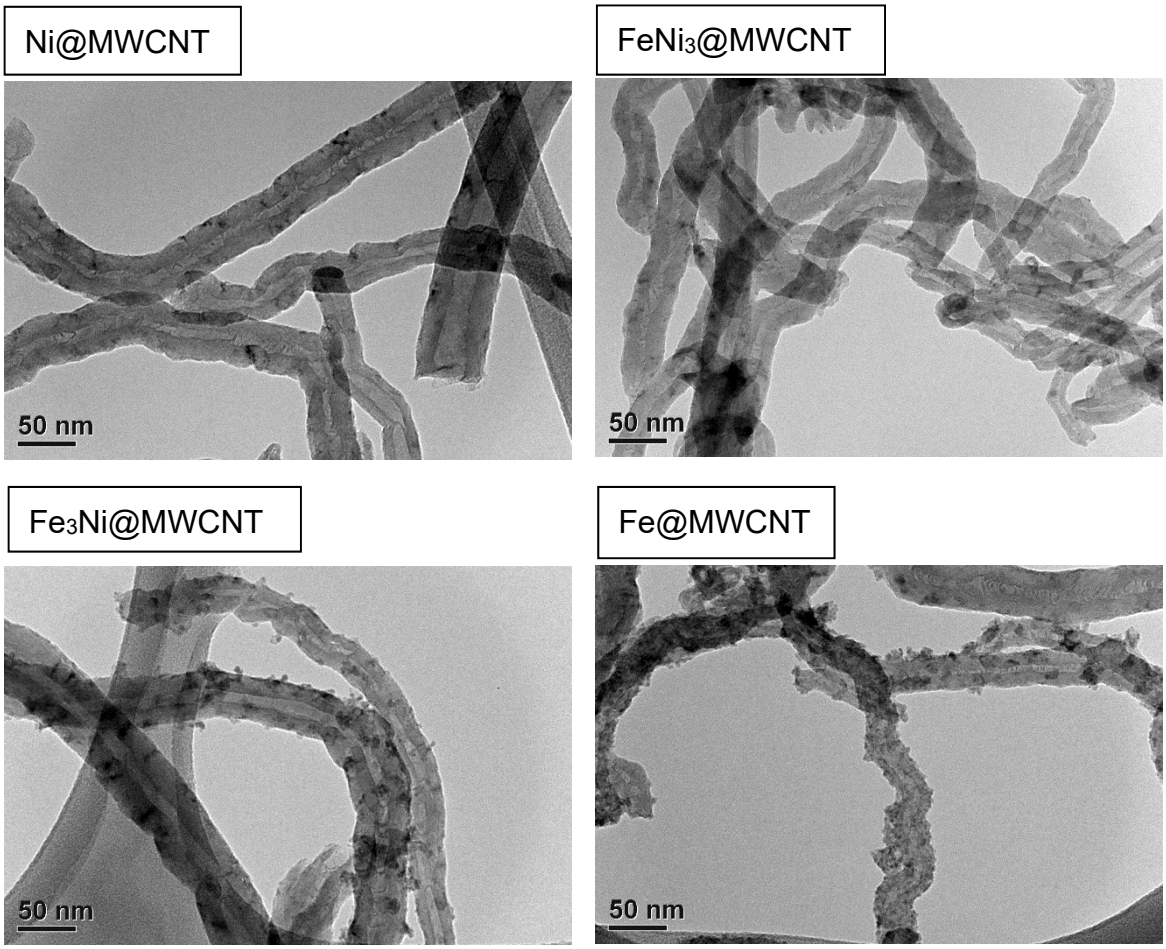


**Fig. S11** TEM images of $(FeNi)_x$@MWCNT including Ni@MWCNT, $FeNi_3$@MWCNT, $Fe_3Ni$@MWCNT, and Fe@MWCNT.

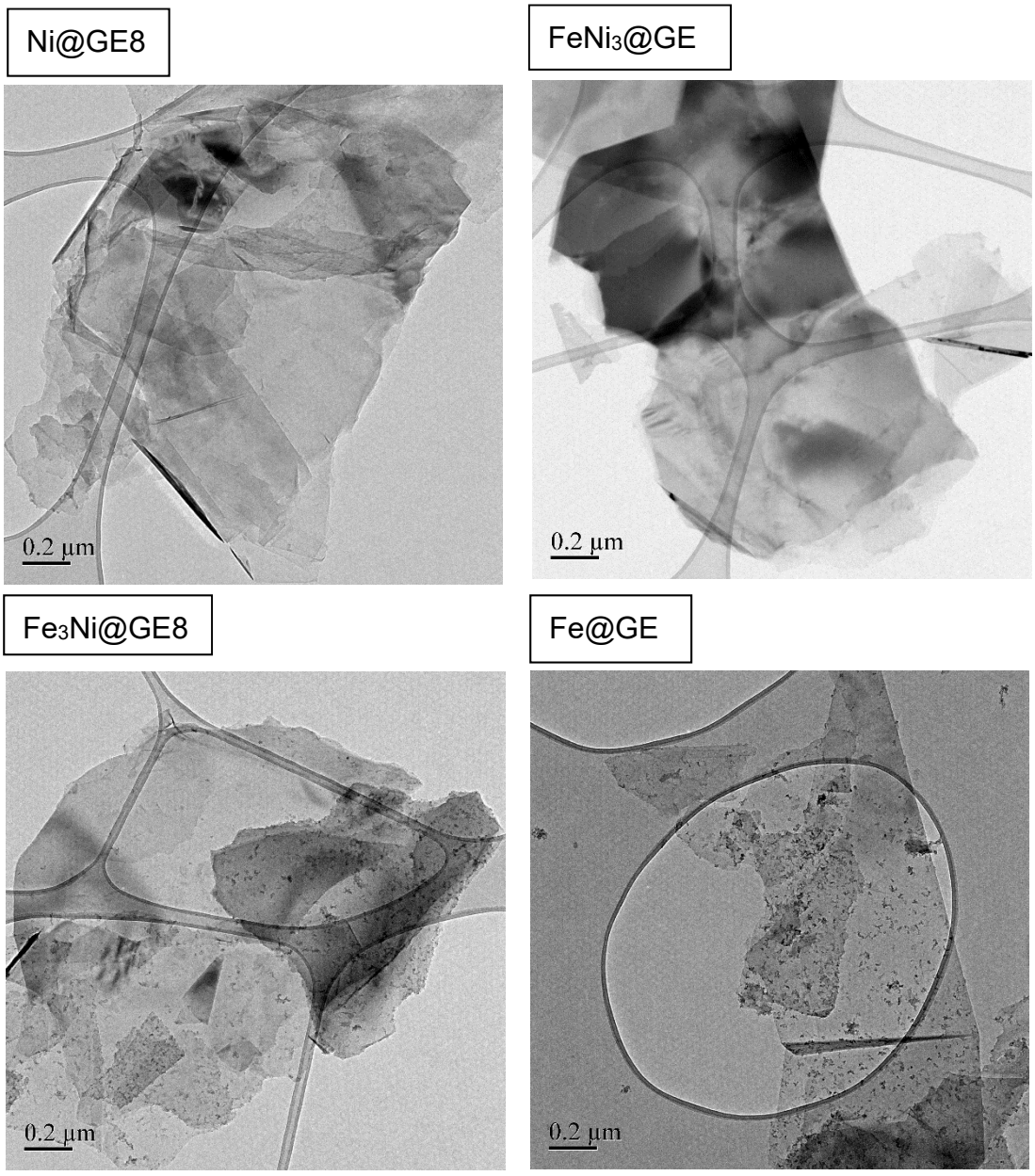


**Fig. S12** TEM images of $(FeNi)_x$@GE8 including Ni@GE8, $FeNi_3$@GE8, $Fe_3Ni$@GE8, and Fe@GE8.

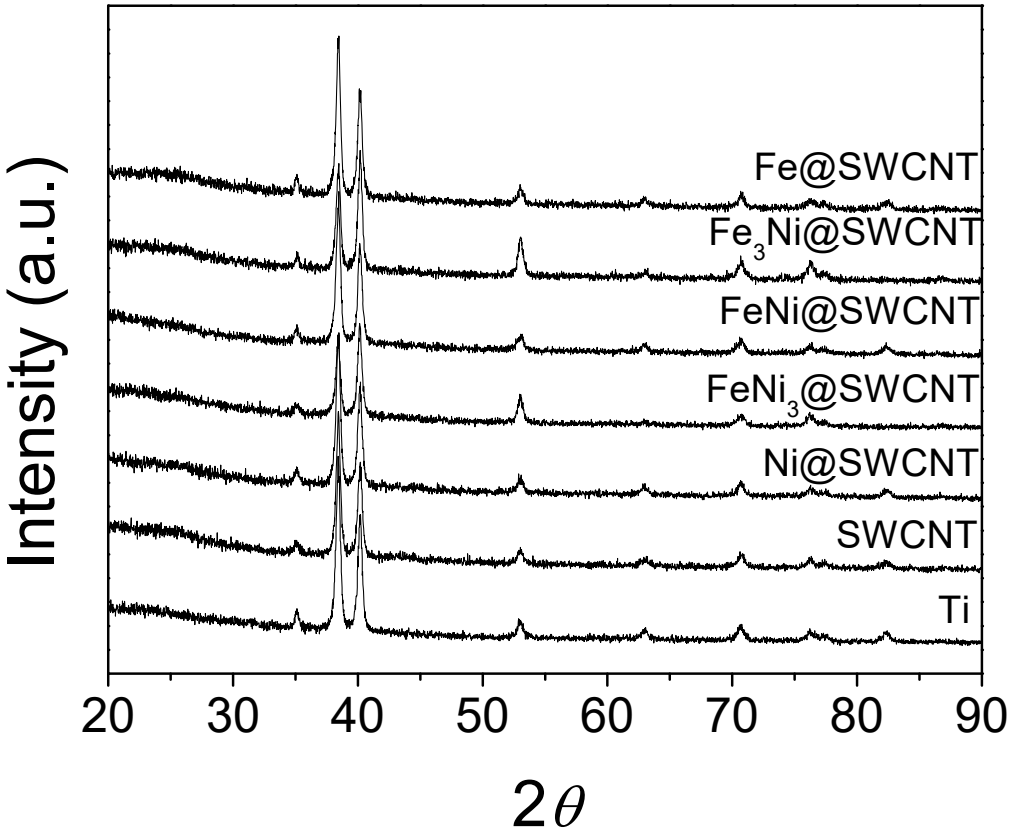


**Fig. 13** X-ray diffraction of $(FeNi)_x$@SWCNT on a Ti sample holder.


**Fig. S14** $FeNi_3$@SWCNT ink loaded in a sprayer can homogeneously spray catalysts onto any conducting substrates for OER application.

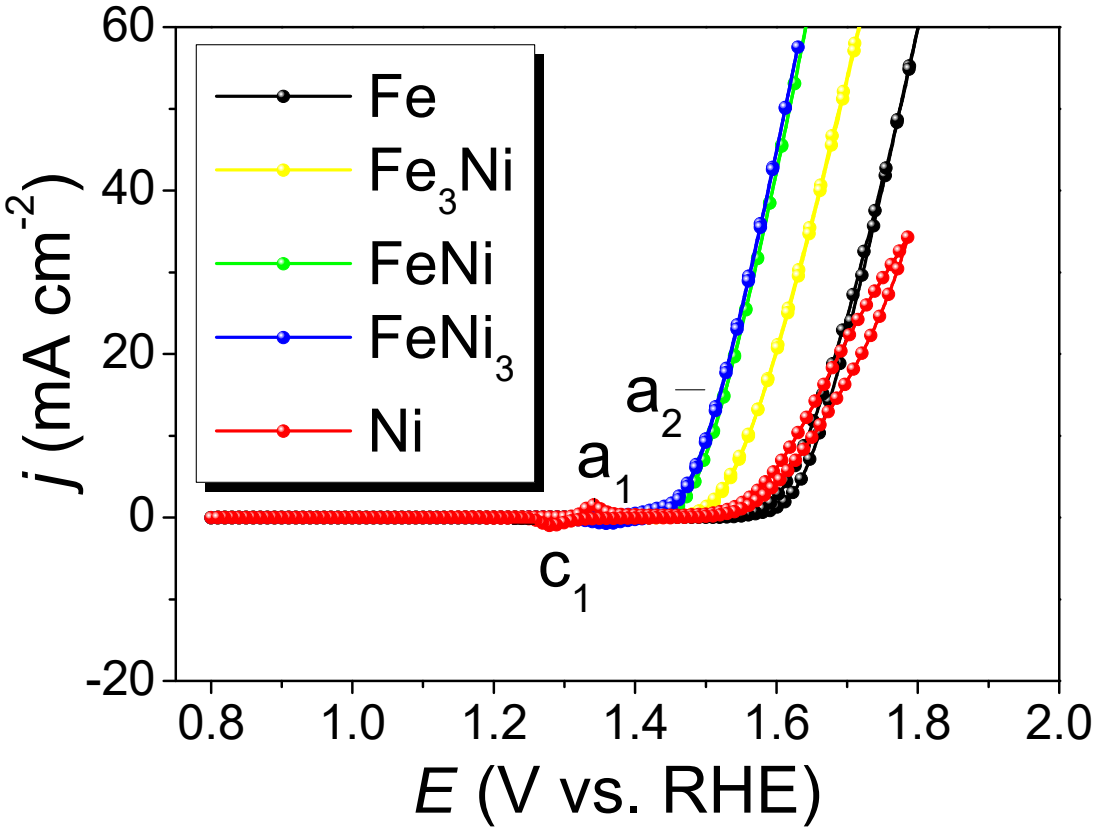


**Fig. S15** OER CVs for the $(FeNi)_x$@SWCNT series recorded in 1.0 M KOH with a scan rate of 10 mV/s.

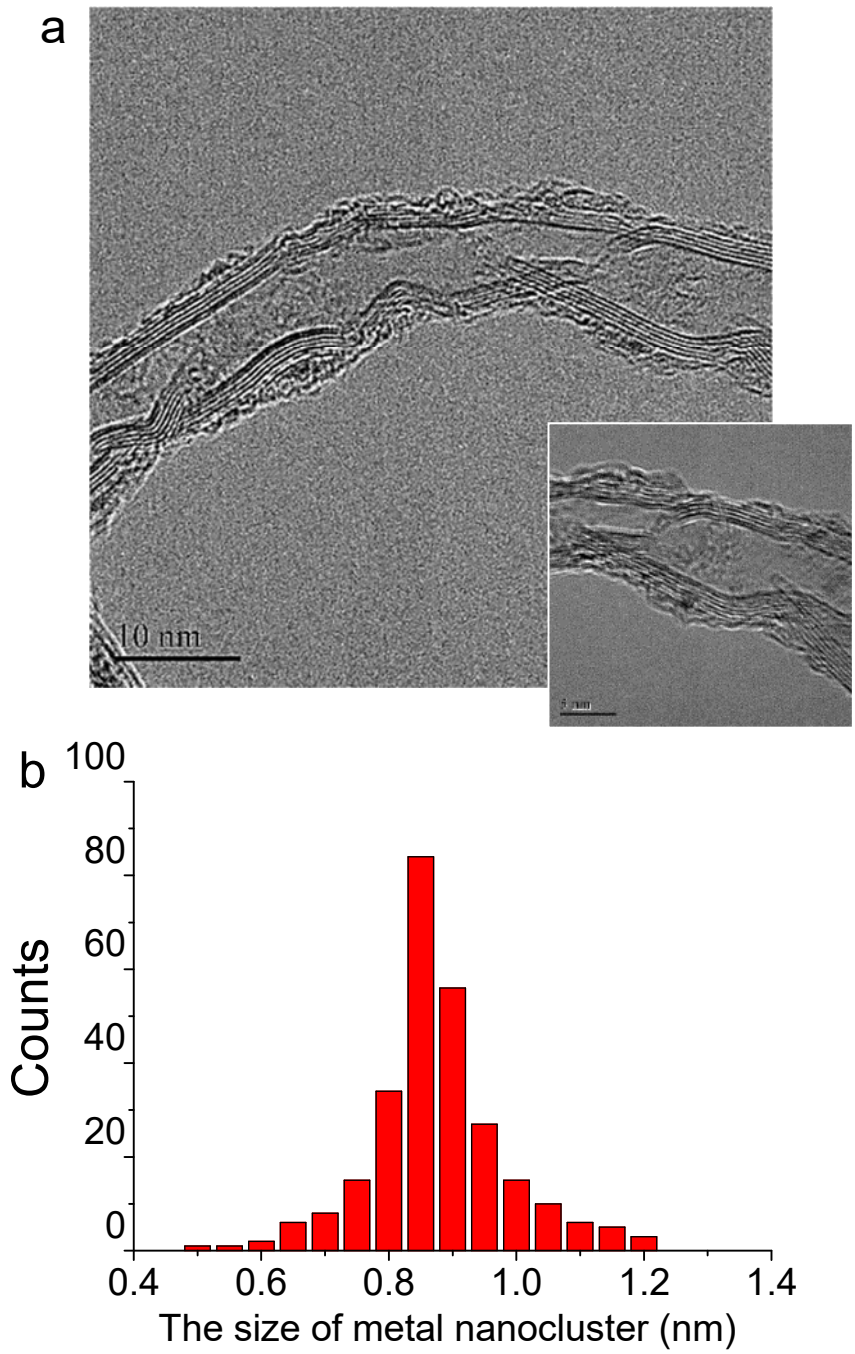


**Fig. S16** HR-TEM images of (a) $FeNi_3$@SWCNT and (b) Histograms of metal nanocluster size constructed by counting 200−300 nanoclusters on the SWCNT in TEM images of $FeNi_3$@SWCNT

**Table S1.** Comparisons of OER performance for various transition metal-based electrocatalysts.

| Catalyst | Catalyst loading | TOF | Tafel slope | $J_m^*$ | $J_m@\eta^*$ | $\eta_{10}^*$ | Refs. |
|---|---|---|---|---|---|---|---|
| | mg $cm^{-2}$ | $s^{-1}$ | mV $dec^{-1}$ | A $mg^{-1}$ | A $g^{-1}$ | V | |
| $FeNi_3$@SWCNT | 0.00042 | 14.03 | 30.2 | 23.81 | 92249.6@0.3V | 0.275 | |
| FeNi@SWCNT | 0.00041 | 8.2 | 31.2 | 24.39 | 53925.8@0.3V | 0.280 | |
| $Fe_3Ni$@SWCNT | 0.00045 | 1.25 | 35.4 | 22.22 | 8247.3@0.3V | 0.329 | this work |
| Fe@SWCNT | 0.00046 | 0.02 | 36.3 | 21.74 | 0.0066@0.3V | 0.442 | |
| Ni@SWCNT | 0.00040 | 0.31 | 46.2 | 25.00 | 0.86@0.3V | 0.360 | |
| $Fe_3Co(PO_4)_4$@rGO | 1.0 | 0.54 | 57 | 0.01 | 0.54@0.237V | 0.237 | [27] |
| NiMoN@NiFeN | 1270 | 0.09 | 58.6 | 0.0079 | 0.163@0.3V | 0.277 | [28] |
| AN-CuNiFe | 0.025 | 3.3 | 44 | 0.4 | 1464.5@0.3V | 0.224 | [26] |
| Au/NiFe LDH | 2 | 0.11 | 36 | 0.005 | 64.9@0.28V | 0.237 | [25] |
| FeP/$Ni_2P$ | 8 | 0.16 | 22.7 | 0.00125 | 159.6@0.3V | 0.154 | [24] |
| $Fe(TCNQ)_2$/Fe | 0.49 | N/A | 110 | 0.0204 | NA | 0.340 | [23] |
| Fe-Co-2.3Ni-B | 0.3 | N/A | 38 | 0.0333 | N/A | 0.274 | [22] |
| $Ni_3Fe_{0.5}V_{0.5}$ | 1.27 | 0.09 | 58.6 | 0.0079 | 0.163@0.3V | 0.264 | [21] |
| Fe-$NiSe_2$ | ~0.2 | 0.071 | 41 | 0.05 | 124.3@0.29V | 0.268 | [20] |
| $Ni_2Fe_1$-O | 0.15 | N/A | 39 | 0.0667 | N/A | 0.244 | [19] |
| Ni@NC-800 | 0.31 | N/A | 45 | 0.0323 | N/A | 0.280 | [18] |
| P-Co3O4 | 0.4 | 0.0158 | 51.6 | 0.025 | N/A | 0.280 | [17] |
| Ultrathin CoFe LDHs | 0.2 | 4.78 | 37.9 | 0.05 | 190@0.3V | 0.266 | [42] |
| Ni45Fe55/XC-72r | 0.01 | 0.2 | 36 | 1 | 2000@0.3V | N/A | [37] |
| NiFe-MOF | N/A | 3.8 | 34 | N/A | N/A | 0.24 | [15] |

| | | | | | | | |
|---|---|---|---|---|---|---|---|
| Gelled FeCoW | 0.21 | 0.46 | N/A | 0.05 | 1175@0.3 | 0.223 | [14] |
| $Fe_{0.5}V_{0.5}$ | 0.143 | 0.02 | 36.7 | 0.07 | 6.99@0.292V | 0.39 | [16] |
| CP/CTs/Co-S | 0.32 | 0.016 | 72 | 0.0313 | 31.3*0.306 | 0.306 | [29] |
| FeOOH/Co/FeOOH | 0.5 | 2.33 | 32 | 0.02 | 40@0.25 | 0.25 | [13] |
| NiFe LDH/GO | 0.25 | 0.1 | 42 | 0.04 | 40@0.23 | 0.23 | [11] |
| NiFe-LDH/CNTs | 0.2 | 0.56 | 31 | 0.05 | 47.63@0.3 | 0.26 | [10] |
| $Ni_{0.75}V_{0.25}$-LDH | 0.143 | 0.054 | 50 | 0.07 | 70@0.35 | 0.35 | [12] |

* $J_m$: Mass activity at 10 mA $cm^{-2}_{geo}$; $J_m@\eta$: Mass activity @specific $\eta$; $\eta_{10}$: Overpotential for 10 mA $cm^{-2}_{geo}$